Elevated atmospheric deposition and dynamics of mercury in a remote upland forest of southwestern China

Xuewu Fu [a], Xinbin Feng [a,*], Wanze Zhu [b], S. Rothenberg [a], Heng Yao [a,c], Hui Zhang [a,c]

[a] State Key Laboratory of Environmental Geochemistry, Institute of Geochemistry, Chinese Academy of Sciences, Guiyang 550002, PR China
[b] Institute of Mountain Hazards and Environment, Chinese Academy of Sciences, Chengdu 610041, PR China
[c] Graduate University of the Chinese Academy Sciences, Beijing 100049, PR China

Upland forest ecosystem is a great sink of atmospheric mercury in southwest China.

ABSTRACT

Mt. Gongga area in southwest China was impacted by Hg emissions from industrial activities and coal combustion, and annual means of atmospheric TGM and PHg concentrations at a regional background station were 3.98 ng m^{-3} and 30.7 pg m^{-3}, respectively. This work presents a mass balance study of Hg in an upland forest in this area. Atmospheric deposition was highly elevated in the study area, with the annual mean THg deposition flux of 92.5 μg m^{-2} yr^{-1}. Total deposition was dominated by dry deposition (71.8%), and wet deposition accounted for the remaining 28.2%. Forest was a large pool of atmospheric Hg, and nearly 76% of the atmospheric input was stored in forest soil. Volatilization and stream outflow were identified as the two major pathways for THg losses from the forest, which yielded mean output fluxes of 14.0 and 8.6 μg m^{-2} yr^{-1}, respectively.

© 2010 Elsevier Ltd. All rights reserved.

1. Introduction

Both anthropogenic and natural activities are sources of mercury (Hg) to the atmosphere. Once emitted into the atmosphere, Hg can be transported a considerable distance and transformed by complex physical and chemical processes. Hg is eventually deposited to the oceans, soils, and lakes, where it may be converted to a more toxic form (e.g. methylmercury), which is bioaccumulated in the aquatic food chain. Generally, industrial and urban areas have high anthropogenic emissions of Hg and are regarded as Hg output areas (Dvonch et al., 1999; Landis and Keeler, 2002; Landis et al., 2004). On the other hand, most remote terrestrial ecosystems, which have much lower Hg emissions and are exposed to great loading of long-range transport Hg from polluted areas, are sinks of atmospheric Hg and have a problem of Hg accumulation (Porvari and verta, 2003; Galloway and Branfireun, 2004; Bushey et al., 2008; Larssen et al., 2008; Selvendiran et al., 2008; Feng et al., 2009a,b). Wet and dry depositions of atmospheric Hg are important sources of Hg to most terrestrial ecosystems. There are three most important species of Hg in the atmosphere, known as gaseous elemental mercury (GEM), reactive gaseous mercury (RGM), and particulate mercury (PHg). Wet deposition results from uptake of RGM and precipitation scavenging of PHg by cloud-droplet (Lindberg et al., 2007), while dry deposition refers to direct depositions of these Hg species to soil, water bodies, and vegetations. In contrast to wet deposition, dry deposition of Hg is difficult to be scaled because of the lack of accurate measurements. In recent years, however, the contribution of dry deposition to the global pool of atmospheric Hg is increasing recognized. One of the most important reasons is the discoveries of the enhancement of dry deposition in canopy covered areas (Lindberg and Stratton, 1998; St. Louis et al., 2001; Poissant et al., 2004).

The forest ecosystem, which covers nearly 1/3 of the Earth's terrestrial surface, is very important in the global biogeochemical cycle of Hg and deserves further study to improve our understanding of Hg dynamics. In general, forest tends to be sinks of atmospheric Hg. This is because vegetation could enhance dry deposition of Hg. Previous studies reported that RGM, PHg and GEM have high deposition velocities to vegetations (Lindberg and Stratton, 1998; Poissant et al., 2004, 2008). Dry deposition of Hg to forest canopy followed by throughfall and litterfall is an additional source of Hg to forest (St. Louis et al., 2001; Rea et al., 2001). On the other hand, vegetation cover could significantly inhibit Hg emission flux from forest soils due to shading of solar radiation, which is crucial in soil/air Hg exchange flux (Coolbaugh et al., 2002; Wang et al., 2007). The addition of Hg to forest system could result

---

* Corresponding author. Tel.: +86 851 5891356; fax: +86 851 5891609. .
  E-mail address: fengxinbin@vip.skleg.cn (X. Feng).

in a series of potential impacts on the biogeochemical cycle of Hg in forest and downstream watersheds. Hg stored in the forest soil may act as a source of both total mercury (THg) and methylmercury (MeHg) to watersheds via mobilization and surface runoff (Munthe et al., 2001). Methylation of Hg in forest soil and decomposed litterfall has also been reported in some forest ecosystem, which has resulted in elevated MeHg concentrations in stream water (Munthe et al., 2001; Hall and St.Louis, 2004; Balogh et al., 2003).

Atmospheric Hg emissions in China are predicted to increase due to fast economic development (Wu et al., 2007). The great anthropogenic emissions have resulted in elevated atmospheric Hg concentrations and depositions in industrial and urban areas (Liu et al., 2002; Feng et al., 2004; Fang et al., 2004), and had the potential to cause Hg pollution in surrounding areas and even remote areas of China via long-range atmospheric transport (Wang et al., 2008; Larssen, 2009). Our previous studies demonstrated that atmospheric TGM (GEM + RGM) concentrations were significantly elevated in Mt. Gongga area even at sites far from human activities due to regional industrial and coal combustion emissions. (Fig. 1, Fu et al., 2008a, 2009). In this paper, we present a study on the inputs and outputs of Hg in an upland forest located in the Mt. Gongga area. From May 2005 to April 2007, we undertook comprehensive field measurements on the distribution of THg and MeHg (MeHg: only in precipitation and throughfall) in precipitation, throughfall, vegetation leaves. By doing this, a preliminary estimation of wet and dry deposition of Hg to this area was calculated. Besides, investigations on output of Hg from the catchment via stream output and emission to the atmosphere were also carried out.

2. Experiments

2.1. Study area

The study area was located in an upland forest catchment at Hailuogou National Forest Park (HNFP, 151.9 km^2) on the eastern slope of Mt. Gongga. Mt. Gongga is situated on the quaternary sections of the eastern Qinghai-Tibet Plateau and its transit zone to the Sichuan Province. It is the highest mountain in Sichuan Province

of southwest China, with the summit of 7556 m above sea level. The HNFP belongs to the subtropics monsoon climate region, with distinct rainy (May to October) and dry (November to April) seasons. Vertical geoecological zonations are well defined in this area, with distinctive climate, vegetation, and soil distributions at different elevations. Mean annual precipitation and humidity generally increases with elevation, while temperature and evaporation decrease. The HNFP is an area with high biodiversity, and an intact and continuous vertical vegetation spectrum from the evergreen broad leaf forest to alpine meadow. Soil types are generally associated with the vegetation spectrum, and yellow brown soil, brown earth, podzolic soil, and alpine meadow soil can be observed gradually with increasing elevation.

2.2. Precipitation and throughfall

Precipitation samples were collected at an open-air site near a meteorological station, which belongs to the Gongga Mountain Alpine Ecosystem station of the Chinese Academy of Science (3000 m a.s.l.). Throughfall samples were collected at two sites. One site was located in an Emei fir forest, and the other was located in a broad leaf Cuculidae forest. The two sites were located within 200 m from the precipitation sampling site. The sampling campaign for precipitation was from May 2005 to April 20 007, and the sampling campaigns for the two throughfall sampling sites were in May 2005–April 2006 and May 2006–April 2007, respectively (Table 1). Precipitation and throughfall samples were collected by using a bulk precipitation collector with an acid-washed borosilicate glass bottle and a borosilicate glass wide-mouthed (15 cm in diameter) jar supported in a PVC housing system (developed from Oslo and Paris Commission, 1998). Precipitation and throughfall samples were both collected weekly during rainy season (April to October). However, during the winter period (November to March), no throughfall samples were collected because of snowfall. In the winter, bulk snow samples were collected monthly by scooping up the upper layer of snow from an open-air site. Landis and Keeler (1997) found that the volume-weighted averages for wet-only events and bulk samples were comparable in a rural site in Dexter
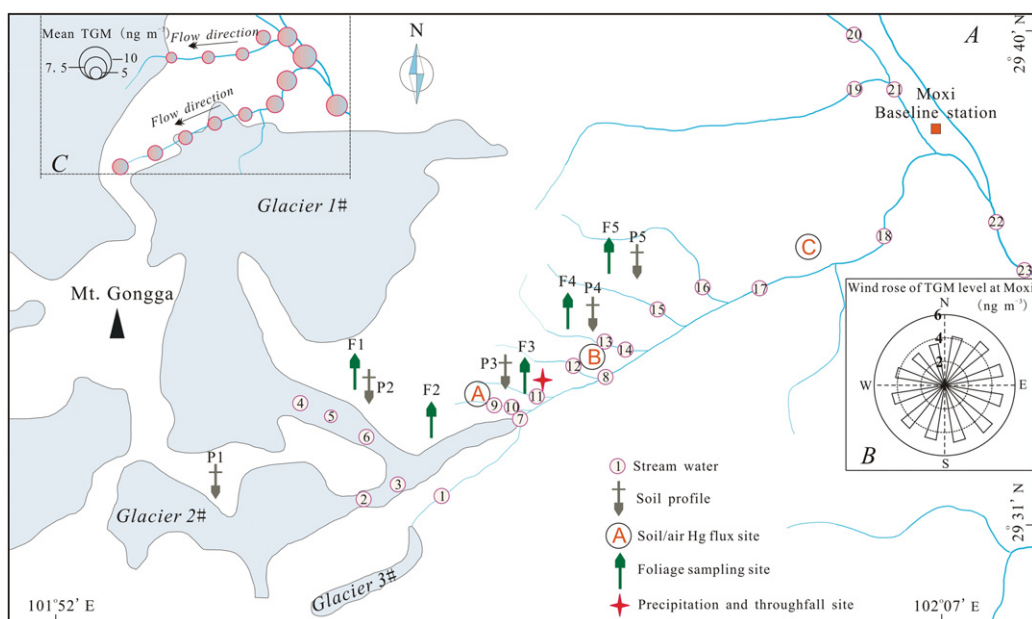

Fig. 1. Map showing (A) Locations of sampling sites, (B) wind rose of annual TGM concentrations at Moxi baseline station and (C) regional distribution of TGM concentrations in Mt. Gongga area in November 2006.

Table 1
Time schedule of the field campaigns.

Sampling		Start time	End time
Precipitation		May 2005	April 2007
Throughfall	Emei fir forest	May 2005	April 2006
	Broad leaf Cuculidae forest	May 2006	April 2007
Vegetation leaves		Aug 22, 2006	Aug 24, 2006
Soil/air Hg flux		Aug 17, 2006	Sep 1, 2006
Glacier melt water and stream water		Jul 16, 2006	Jul 19, 2006
Soil profile		Sep 10, 2006	Sep 11, 2006

of east USA. In the study area (Fu et al., 2008b), however, the PHg concentrations (mean: 30.7 pg m^{-3}) were slightly higher and RGM concentrations (mean: 6.2 pg m^{-3}) were comparable to rural sites in North America (Valente et al., 2007, and references therein). Hence, our bulk sampling method might slightly overestimate precipitation and throughfall Hg concentrations.

The collected rain samples were transported in rigorously acid-cleaned Teflon bottles (250 ml) and preserved by adding trace-metal grade HCl (to 5‰ of total sample volume). All Teflon bottles were cleaned with detergent, thoroughly rinsed with tap water, boiled in a 30% HNO$_3$ solution (v/v) for 1.5 h and rinsed and filled with Milli-Q water. During all sampling, polyethylene gloves were employed. Teflon bottles with samples were individually sealed into three successive polyethylene bags and rapidly brought to the laboratory and stored in a refrigerator until analysis. Rainfall was measured in the nearby meteorological station. The throughfall depth was measured by using a graduated cylinder as soon as possible after precipitation events.

2.3. Vegetation leaves

Fresh and intact leaves were sampled at five locations in HNFP in late August 2006 (Table 1). Elevations of the five sampling sites F1, F2, F3, F4, and F5 were 2650, 2800, 3000, 3200, and 3580 m above sea level, respectively (Fig. 1). At each location, six main types of vegetation, including Grossulariaceae, Maple, Mountain ash, Emei Fir, Broad leaf Cuculidae, and woolly foliage Cuculidae were collected. To obtain representative samples at the sampling sites, three individuals of each type of vegetation were sampled. Leaves were collected from branches by selecting fully developed undamaged leaves, which were stored in brown paper bags, and air-dried in a clean environment in the laboratory until analysis.

2.4. Evasion flux of Hg from soil

Evasion fluxes of Hg from forest soil were determined by using a coupling method of dynamic flux chamber and automated air Hg analyzer (Tekran 2537A). Hg flux over the soil surface enclosed by the chamber was calculated according to the following equation:

$$F = (C_o - C_i) \times Q/A \tag{1}$$

where F is the TGM flux in ng m^{-2} h^{-1}; C_o and C_i are the TGM concentrations of the outlet and inlet air stream in ng m^{-3}; A is the surface area enclosed by the chamber in m^2 (0.06 m^2); and Q is the flushing flow rate through the chamber in m^3 h^{-1} (0.6 m^3 h^{-1}). TGM concentrations were measured twice in the ambient air entering the inlet of the chamber and twice in the air exiting through outlet of the chamber using an automated air Hg analyzer (Tekran 2537A) with a 5 min sampling interval. Switching from the inlet to the outlet of the chamber every 10 min was achieved by using a magnetic 3-way valve (Tekran 1110). Another mass flow controller combined with the second magnetic 3-way valve, which was synchronous with the first one, was employed to compensate flow rate decrease when the

Tekran was sampling air from the inlet of the chamber. A high flushing flow rate of 10 L min^{-1} (0.6 m^{-3} h^{-1}) was adopted to prevent the possibility of underestimating Hg flux at low flushing flow rates (Gillis and Miller, 2000; Zhang et al., 2002; Lindberg et al., 2002). Blanks of the flux sampling system were routinely measured by placing the chamber on a Quartz glass surface and fell in the range of 0.06–0.13 ng m^{-2} h^{-1}, the blanks were small and we did not make blank correction for measured fluxes.

Hg flux measurements were monitored at three sampling sites in the upland forest in HNFP during Aug 17 and Sep 1 in 2006 (Fu et al., 2008c). The three sampling sites were located in evergreen broadleaved forest (1650 m, yellow brown earth), coniferous and deciduous broadleaved mixed forest (2140 m, brown earth), and dark coniferous forest (3050 m, dark brown soil), respectively (Fig. 1). During each sampling campaign, air/soil Hg exchange fluxes were measured continuously for more than 24 h to obtain diurnal patterns.

2.5. Glacier melt water and stream water

The Hailuogou River is the main output channel with tributary streams in the HNFP originating from glacier melt water. Glacier melt water and stream water samples were collected from 23 sampling sites as shown in Fig. 1 from 16 to 19 July 2006. Water samples were colleted in rigorously pre-cleaned 250 ml Teflon bottles. For sample collection, bottles were rinsed three times with the water samples before being filled. Samples were not filtered and thus represent the stream load of total Hg. The water samples were immediately acidified by adding trace-metal grade HCl (to 5‰ of total sample volume). During all sampling, polyethylene gloves were worn. Teflon bottles with samples were individually sealed into three successive polyethylene bags. All water samples were stored at 4 °C in a refrigerator immediately after being transported to the laboratory.

2.6. Soil profile

The main soil types in the study area are yellow brown earth, brown earth, dark brown soil, and alpine meadow soil, which are distributed continuously from lower altitude to high altitude. Five soil profiles were chosen in the study area along the Hailuogou Valley as shown in Fig. 1. P1 (4200 m a.s.l.) was located in an alpine meadow zone with soil type of alpine meadow soil. P2 (3500 m a.s.l.) was located in dark coniferous forest with brown earth. P3 (3000 m a.s.l.) was located in coniferous and broad-leaf mixed forest with dark brown soil. P4 (2700 m a.s.l.) and P5 (2600 m a.s.l.) were located in warm-temperate, mixed coniferous and broad leaf forest with brown soil. Top soil samples as well as soil samples at 4, 8, 12, 16, and 20 cm in depth were collected, respectively. Soil samples were collected in polyethylene bags using polyethylene gloves and air-dried in a clean environment in the laboratory until analysis.

2.7. Analytical methods

Total Hg concentration in water samples was analyzed using BrCl oxidation and SnCl$_2$ reduction coupled with CVAFS detection (US EPA, 1999). MeHg concentration in water samples was analyzed via distillation, aqueous ethylation, purge and trap, and detected by CVAFS (US EPA, 2001). For THg analysis in soil and leaf tissue samples, 0.1–0.2 g dry sample were digested in a water bath at 95 °C, with BrCl and mixed acid of HCl/H$_2$SO$_4$ (3 : 1 in volume)and HNO$_3$/H$_2$SO$_4$ (8 : 2 in volume), respectively. Mercury concentration in digested solution was then analyzed via reduction, purge and trap, and CVAFS (US EPA, 2001).

Total organic Carbon (TOC) content in forest soil was estimated by using the sequential loss on ignition (LOI) (Heiri et al., 2001; De Vos et al., 2005; Westman et al., 2006). An air-dried soil sample (WS) was dried at 105 °C for about 12–24 h to obtain the dry weight of the samples (DW$_{105}$). The heated dry sample was then burned at 550 °C for 4 h and the weight of the sample after heating at 550 °C was DW$_{550}$. Thus, LOI$_{550}$ was calculated according to the following equation:

$$LOI_{550} = 100(DW_{105} - DW_{550})/WS \qquad (2)$$

Quality assurance and quality control of the analytical processes were addressed with method blanks, field blanks, blind duplicates, matrix spikes, and certified reference materials. Filed blanks and duplicates were collected regularly throughout each sampling campaign ($\sim$10% of samples). Detection limits were based on three times the standard deviations of blank measurements. Field blank levels for THg and MeHg in water samples were 0.5 ng L^{-1} and 0.03 ng L^{-1}, respectively. The method detection limits for THg and MeHg in water samples and THg in soil and leaf tissue were 0.02 ng L^{-1}, 0.01 ng L^{-1}, 0.01 mg kg^{-1}, and 0.006 mg kg^{-1}, respectively. Precision was determined by relative standard deviations (RSDs) for duplicate samples, which were 6% for THg analysis in water samples, 5.4% for MeHg analysis in water samples, 8% for THg analysis in soil samples, and 3.9% for THg analysis in leaf tissues. Recoveries on matrix spikes of MeHg in water samples were in the range of 87–110%. The measured THg concentrations in certified reference soil (GWB07405) and vegetation (Rice, GWB10010) were finally averaged to be 0.27 μg g^{-1} and 5.8 ng g^{-1}, respectively, which were comparable to the certified values of 0.29 μg g^{-1} and 5.3 ng g^{-1}, respectively.

3. Result and discussion

3.1. Concentrations and deposition fluxes of precipitation and throughfall

Monthly volume-weighted mean concentrations of THg and MeHg in precipitation and deposition fluxes are presented in Fig. 2. We obtained a continuous data set of MeHg concentrations from June 2005 to October 2006. For other months, analysis of MeHg in precipitation was not available because of the lack of samples. Generally, no consistent seasonal variation of THg and MeHg concentrations was observed during the two years of sampling. The highest THg concentration was observed in the winter of 2006, while the highest concentration of MeHg was observed in the winter of 2005.

Hg concentrations and estimated Hg deposition fluxes for precipitation and throughfall are presented in Table 2. THg concentrations in precipitation varied from 6.9 to 46.3 ng L^{-1} and had an overall volume-weighted mean concentration of 14.3 ng L^{-1} during the whole sampling campaign. Concentrations of MeHg in precipitation ranged from 0.05 to 0.39 ng L^{-1}, and the overall volume-weighted MeHg concentration was 0.16 ng L^{-1}. Generally, the MeHg concentration in precipitation was 1.1% of THg, which was comparable to results from Europe and North America (St. Louis et al., 2001; Hall et al., 2005; Lindberg et al., 2007).

Monthly variations of THg and MeHg concentrations and deposition fluxes in throughfall in the two forests are shown in Fig. 3. Volume-weighted mean THg concentrations in the throughfall of Emei fir and broad leaf Cuculidae forests were 37.0 ng L^{-1} (monthly means varied from 18.3 to 49.2 ng L^{-1}) and 43.6 ng L^{-1} (monthly means varied from 24.4 to 62.0 ng L^{-1}), respectively. Volume-weighted mean MeHg concentrations were 0.35 ng L^{-1} (monthly means ranged from 0.20 to 0.51 ng L^{-1}) and 0.21 ng L^{-1} (monthly
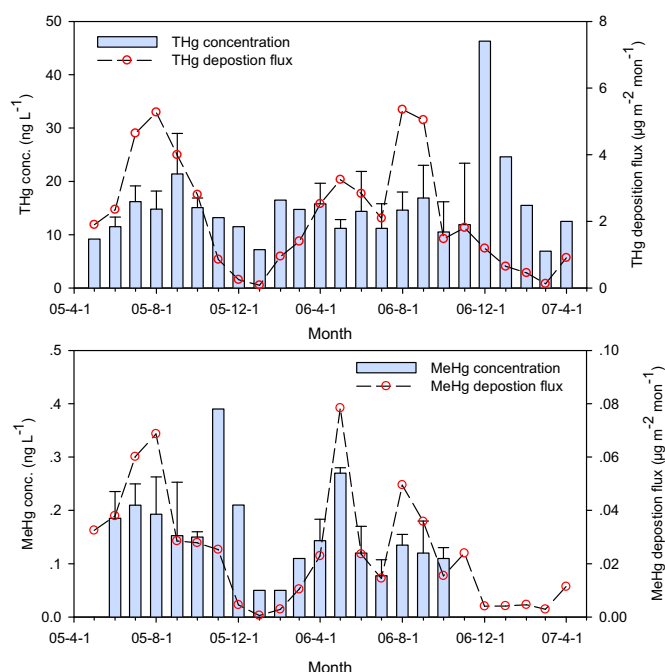

Fig. 2. Monthly volume-weighted mean concentrations of THg and MeHg and deposition fluxes of precipitation in the upland forest of HNFP from May 2005 to April 2007.

means varied from 0.18 to 0.32 ng L^{-1}), respectively. Differences in THg and MeHg concentrations between precipitation and throughfall were statistically significant (Emir fir forest: $p_{THg} = 0.001$, $p_{MeHg} = 0.013$; Broad leaf Cuculidae forests: $p_{THg} = 0.002$, $p_{MeHg} = 0.037$). The elevated THg and MeHg concentrations in throughfall samples were probable attributed to the wash-off of Hg previously deposited to vegetation leaves.

Generally, volume-weighed mean THg and MeHg concentrations in precipitation and throughfall in the HNFP were much lower compared to some polluted sites in China, such as: Wujiang River Basin, Guizhou province (precipitation: THg: 36.0 ng L^{-1}; MeHg: 0.18 ng L^{-1}, Guo et al., 2008); Leigongshan, Guizhou province (precipitation: THg: 19.5 ng L^{-1}; throughfall: THg: 54.2 ng L^{-1}, Wang et al., 2008), Tieshanping, Chongqing city (precipitation: THg: 55.3 ng L^{-1}; throughfall: THg: 98.9 ng L^{-1}, Wang et al., 2008). This is mainly because the study area was relatively isolated from direct anthropogenic Hg emissions. However, the volume-weighed mean THg and MeHg concentrations in precipitation and throughfall in the study area were much higher ($\sim$1.5–2 folders higher) than those observed in remote areas of North America and Europe, which were generally less than 10 ng L^{-1} for precipitation and less than 30 ng L^{-1} for throughfall (St. Louis et al., 2001; Keeler et al., 2005; Choi et al.,

Table 2
Hg concentrations and annual mean Hg deposition fluxes in precipitation and throughfall in HNFP from May 2005 to April 2007.

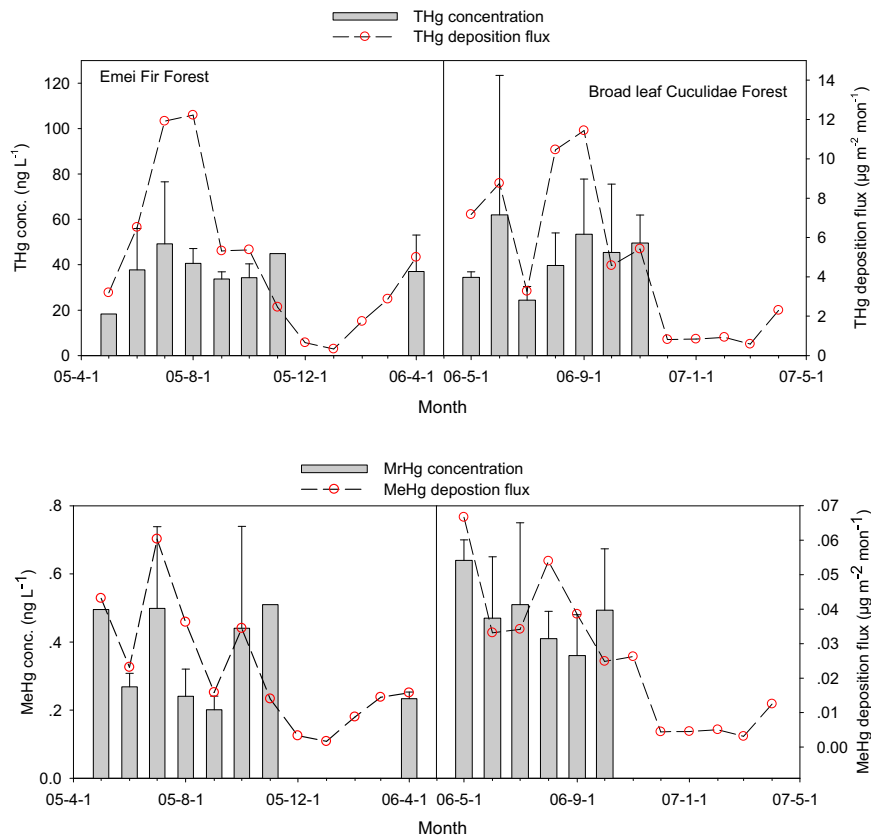|	Rainfall (mm)	Volume-weighted mean concentration		Annual mean deposition flux	
		THg (ng L^{-1})	MeHg (ng L^{-1})	THg (μg m^{-2})	MeHg (μg m^{-2})
Precipitation	1818	14.3 ± 7.7	0.16 ± 0.08	26.1	0.30
Throughfall (Emei fir forest)	1550	36.8 ± 9.2	0.36 ± 0.14	57.6	0.54
Throughfall (broad leaf Cuculidae forest)	1294	43.6 ± 12.5	0.24 ± 0.05	56.5	0.31

Fig. 3. Monthly volume-weighted mean concentrations of THg and MeHg and deposition fluxes of throughfall in Emei fir forest and Broad leaf Cuculidae forest in the upland forest of HNFP from May 2005 to April 2007.

2008; Graydon et al., 2009; Lindberg et al., 2007; US National atmospheric depostion program, 2007).

Levels of atmospheric Hg, especially PHg and RGM, play the most important role in regulating atmospheric Hg depositions (Lindberg et al., 2007; Lee et al., 2001; Seigneur et al., 2003). The study area was heavily impacted by industrial emission of Hg. According to our previous studies, nor-ferrous smelting activities in Shimian city which is located about 60 km from our sampling site were the main sources of atmospheric Hg in Mt. Gongga area, which released nearly 8 tons of Hg to the atmosphere annually (Fu et al., 2008a). This source together with coal combustion resulted in elevated TGM (annual mean: 3.98 ng m^{-3}) and PHg (annual mean: 30.7 pg m^{-3}) concentrations in the study area at a relatively lower elevation site (Moxi regional baseline station, in Fig. 1, Fu et al., 2008a). During daytime, upslope valley breeze that brought Hg polluted air from the industrial and urban areas was the predominant source of Hg in the study area. As seen from Fig. 1, TGM concentrations in the study area during cold season were highly elevated (4.6–7.8 ng m^{-3}) and showed a clear increase from rural sites to residential areas and industrial area (Fu et al., 2009), indicating loading of atmospheric Hg from industrial and urban areas to the sampling site. Hence, it is speculated that cloud-droplet uptake of Hg in regional atmosphere, precipitation scavenging and foliar uptake of RGM and PHg that directly delivered to the sampling sites from industrial and urban areas or transformed from Hg^0 by oxidation contributed significantly to the elevated precipitation and throughfall THg concentrations in the study area.

Deposition fluxes of THg and MeHg in precipitation and throughfall were estimated using the volume-weighed mean concentrations and the annual rainfall (Table 2). Average deposition fluxes of THg and MeHg in precipitation were 26.1 μg m^{-2} yr^{-1} and 0.30 μg m^{-2} yr^{-1}, respectively. Due to the high concentrations of THg in throughfall, deposition fluxes of THg in throughfall in the two upland forests were highly elevated compared to precipitation. The throughfall deposition fluxes of THg in the Emei fir and broad leaf Cuculidae forests were 57.6 and 56.4 μg m^{-2} yr^{-1}, respectively. Deposition fluxes of MeHg in throughfall in the Emei fir forest and broad leaf Cuculidae forests were 0.54 and 0.31 μg m^{-2} yr^{-1}, respectively. Throughfall flux of MeHg in the broad leaf Cuculidae forest was comparable to the precipitation flux, and this was because the rainfall depth of precipitation was much higher than that in throughfall (Table 2).

Precipitation and throughfall fluxes of THg in the study area were lower compared to those reported from a few sites in Guizhou, southwestern China (Feng et al., 2009a; Guo et al., 2008; Wang et al., 2008), but were about 2–10 time higher compared to those observed from remote areas in North America and Europe (Precipitation: 3.1–11.6 μg m^{-2} yr^{-1}, throughfall: 4.5–15.8 μg m^{-2} yr^{-1}, St. Louis et al., 2001; Porvari and Verta, 2003; Keeler et al., 2005; US National atmospheric depostion program, 2007; Choi et al., 2008; Graydon et al., 2009). As discussed above, great regional emissions of Hg from industrial activities and coal combustion might be responsible for the great loading of Hg to the upland forest.

The THg fluxes in throughfall were more than two times higher than precipitation, and the net throughfall fluxes (throughfall flux – precipitation flux) in the Emei fir and broad leaf Cuculidae forest were 31.5 and 30.3 μg m^{-2} yr^{-1}, respectively. The net throughfall fluxes of THg in the study area were much higher than those observed from remote forest catchments in North America and Europe (Munthe et al., 1995; St. Louis et al., 2001; Choi et al., 2008;
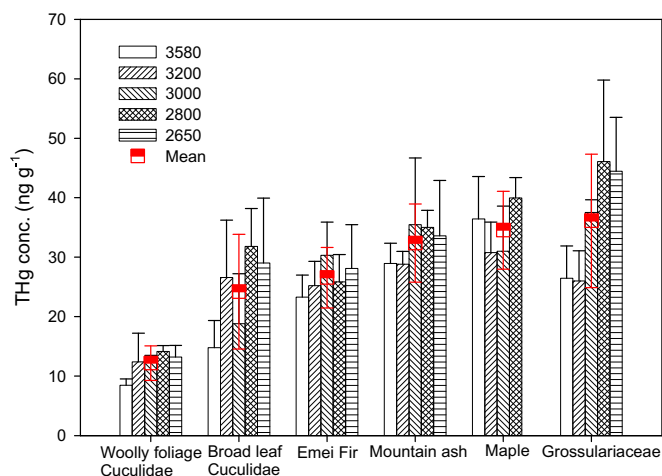
Fig. 4. Variation of THg concentrations in different vegetation species.

Graydon et al., 2009). The elevated net throughfall fluxes of THg indicated that the dry depositions of atmospheric PHg and RGM to the upland forest of HNFP were very high, and this was probably attributed to the contamination of Hg in the regional ambient air due to anthropogenic emissions.

3.2. THg in fresh vegetation leaves and estimation of litterfall deposition flux

THg concentrations in fresh leaves showed a significant variation among vegetation species in the HNFP ($p = 0.002$) (Fig. 4), including Grossulariaceae (36.1 ± 11.2 ng g^{-1}), Maple (34.5 ± 34.5 ng g^{-1}), Mountain ash (32.4 ± 6.6 ng g^{-1}), Emei Fir (26.6 ± 5.1 ng g^{-1}), Broad leaf Cuculidae (24.2 ± 9.6 ng g^{-1}), woolly foliage Cuculidae (12.2 ± 2.9 ng g^{-1}), which were listed in descending order. Besides, THg concentrations in leaf tissue showed a clear difference with elevation variation (Table 3, $p = 0.009$) with higher concentrations at the relatively lower elevation sampling sites (Table 3). Previous study by Stamenkovic and Gustin (2009) suggested that uptake of Hg by foliage via stomatal and nonstomatal pathways could be enhanced by elevated atmospheric Hg concentrations. In this study, atmospheric TGM concentrations showed a similar spatial trend with foliar Hg concentrations (Fig. 1), suggesting it might be partially responsible for the variation in foliar Hg concentrations with elevation. However, some other factors such as vegetation types related to elevations may also correspond to variation of foliar THg concentrations at different elevations.

Numerous studies have demonstrated that uptake of atmospheric Hg followed by litterfall is an important source of Hg in forest system. Here, we made a crude estimation of litterfall

deposition of Hg. Previous studies found that THg concentration in leaf is accumulated continuously over time (Rea et al., 2004; Bushey et al., 2008; Poissant et al., 2008; Selvendiran et al., 2008). Bushey et al. (2008) and Poissant et al. (2008) found that THg concentration in leaves was linearly correlated with time during the gowning season. Generally, the growing season in this area was from the middle of April to the middle of October (6 months), and the sampling period of leaves in this study was in the late August 2006 (Table 1). Assuming THg concentrations in leaves accumulated linearly over the growing season, we approximately estimated litterfall THg concentrations in the study area by multiplying the measured leaves THg concentrations by a factor of 1.5 (Table 3). Litter mass deposition fluxes in the study area were comprehensively investigated by Luo et al. (2000) and shown in Table 3. The estimated litterfall Hg deposition fluxes are shown in Table 3. In total, the mean THg deposition flux of litterfall in the HNFP was estimated to be 35.5 μg m^{-2} yr^{-1}, which is higher than those reported in forest ecosystems from Ontario, Canada (St. Louis et al., 2001), Michigan, USA (Rea et al., 2001), New York state, USA (Bushey et al., 2008). However, it should be pointed that our estimations have many uncertainties and might be a qualitative assessment. First, there might be inter-annual variability in litter mass deposition fluxes. Besides, litterfall Hg concentrations were probably over or under-estimate because accumulation of Hg in vegetations with time could be more complicated and different vegetation species also have distinct characteristics in their growth.

3.3. Hg evasion from forest soil

A clear diurnal pattern of Hg fluxes was obtained from all sites as shown in Fig. 5, with the maximum Hg fluxes observed in the afternoon and minimum Hg fluxes observed during the nighttime. Overall, net evasions were observed from all sampling sites, and only two data sets out of 296 data sets were observed with Hg deposition (Fig. 5). Average fluxes of Hg at sites A, B, and C were 9.3 ± 4.3 ng m^{-2} h^{-1}, 7.7 ± 3.4 ng m^{-2} h^{-1}, and 2.9 ± 2.0 ng m^{-2} h^{-1}, respectively. Soil Hg fluxes in HNFP during the warm season were comparable with Hg fluxes in the forest of Chongqing city, China (Wang et al., 2006), but they were elevated compared to Hg fluxes reported from North America and Europe, such as northern Sierra Nevada Mountains in California (0.3 ± 0.1 ng m^{-2} h^{-1}, Ericksen et al., 2006), Tahquamenon River watershed in the Michigan Upper Peninsula (0.2–2.4 ng m^{-2} h^{-1}, Zhang et al., 2001), and Kejimkujik National Park, Nova Scotia (−0.8–3.5 ng m^{-2} h^{-1}, Boudala et al., 2000).

Emission of Hg from soil is an important pathway for Hg losses from landscapes. However, it is still difficult to accurately quantify the magnitude of the emission of Hg from the study area because soil/air exchange flux of Hg was controlled by multiple interacting factors including substrate Hg content and physical-chemical factors (soil temperature and moisture, soil porosity, soil organic matter etc.), surface characteristics (e.g. bare or vegetation cover),

Table 3
THg concentrations in vegetation leaves and litterfall deposition flux of THg in the upland forest of HNFP.

Site	Altitude (m a.s.l)	THg concentration (ng g^{-1})	Weighted mean Concentration[a] (ng g^{-1})	Annual litter mass (g m^{-2}) (Luo et al., 2000)	Estimated litterfall THg concentration (ng g^{-1})	THg flux (μg m^{-2} yr^{-1})
F1	3580	23.0 ± 10.2	19.3	469	29.0	13.6
F2	3200	25.0 ± 7.7	21.4	1293	32.1	41.4
F3	3000	27.6 ± 10.9	26.0	1133	39.0	44.1
F4	2800	32.1 ± 11.9	25.8	1007	38.7	39.1
F5	2650	29.7 ± 12.6	26.6	985	39.9	39.5
Total mean		27.5 ± 3.6	23.8 ± 3.3	9.8 ± 3.1	35.7	35.5

[a] Weighted mean concentration $= \sum_{i=1}^{i=6}(C_i \times P_i)$, where C_i is the mean THg concentration in foliage of each vegetation species, and P_i is the percentage of each vegetation species in forest.
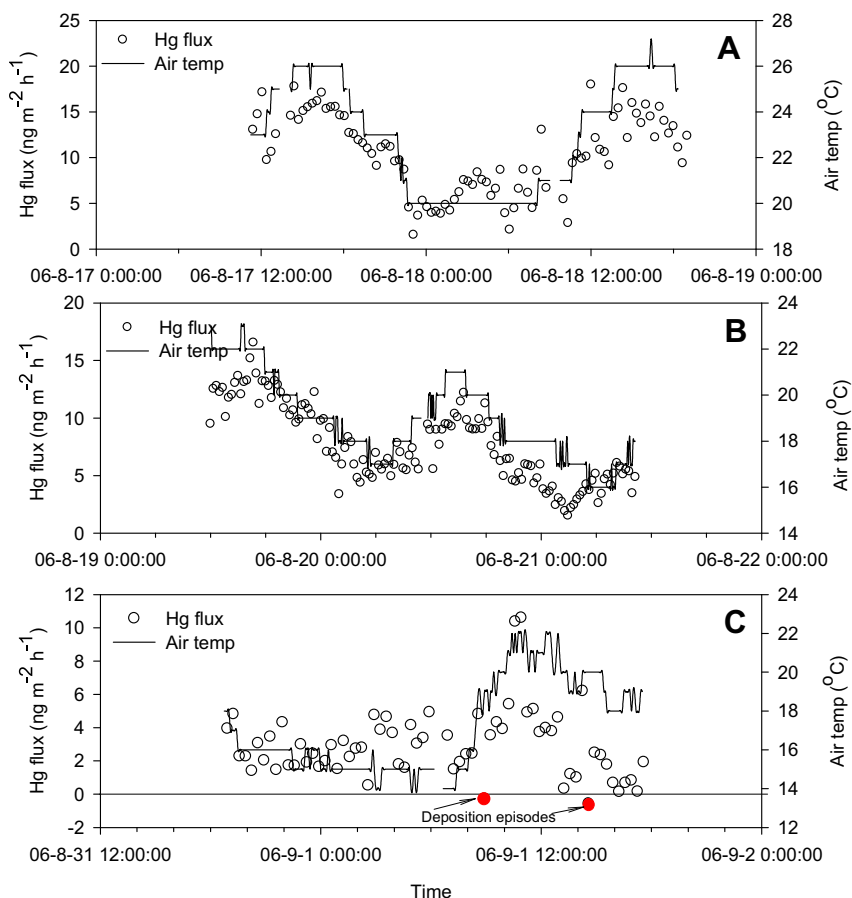
Fig. 5. Soil emission fluxes of Hg and air temperature in the upland forest of HNFP.

and meteorological parameters (e.g. solar radiation, air temperature) (Schroeder et al., 2005; Hartman et al., 2009). Here, a simple attempt is made to estimate the emission of Hg from forest soil using an empirical model developed from our measurements in warm season. As depicted in Fig. 6, a significant relationship between Hg emission flux and air temperature was observed, and this agrees very well with the study in the forest floor of the Adirondacks (Choi and Holsen, 2009). Since air temperature could be easily determined and evenly distributed in the study area, it was used to predict the soil emission of Hg in the study area. The earth's surface was often covered by snow during December and March. According to the study by Schroeder et al. (2005), Hg emission from snow covered surface was extremely low. Therefore, we assumed surface emission of Hg during December and March to be zero. For other months, the average air temperature was ~12.0 °C (mean of air temperatures at two meteorological stations located at the elevations of 1640 and 3000 m a.s.l.). Hence, the annual averaged surface emission flux of Hg was calculated to be 1.6 ng m^{-2} h^{-1}, and this yielded a annual total net Hg emission flux of 14.0 μg m^{-2} yr^{-1}.

3.4. Glacier melt water and stream water

Variation of un-filtered THg concentrations in glacier melt water and steam water in the HNFP is shown in Fig. 7. THg concentrations varied between 1.9 and 5.7 ng L^{-1}, with an overall average concentration of 3.5 ± 0.9 ng L^{-1}. The melting of the glacier at the top of Mt. Gongga area was the major water source of the stream. Samples No 1 to 6 were collected from glacier melt water, and THg concentrations

of these samples ranged from 1.9 to 4.1 ng L^{-1} (mean: 3.19 ng L^{-1}). The glacier melt water THg concentrations were significantly higher than those reported from Antarctica (0.44–1.90 ng L^{-1}, Vandal et al., 1998; Lyons et al., 1999), which was probable attributed to the great atmospheric Hg depositions. Besides, soil erosion and runoff were also additional sources to stream water. THg concentrations in stream water (3.60 ng L^{-1}) were slightly higher compared to glacier melt water, which was probably derived from soil erosion and runoff during stream transport.
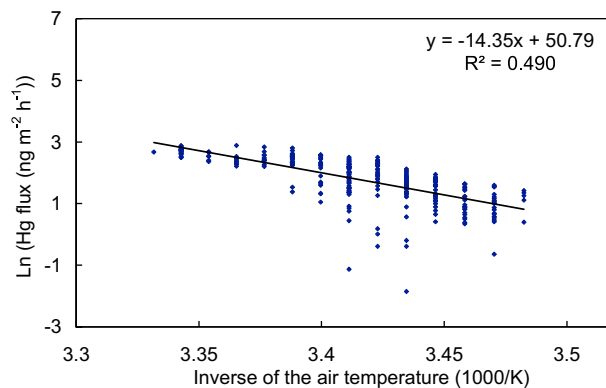

Fig. 6. Arrhenius relationship between Hg flux and air temperature at all the sampling sites.
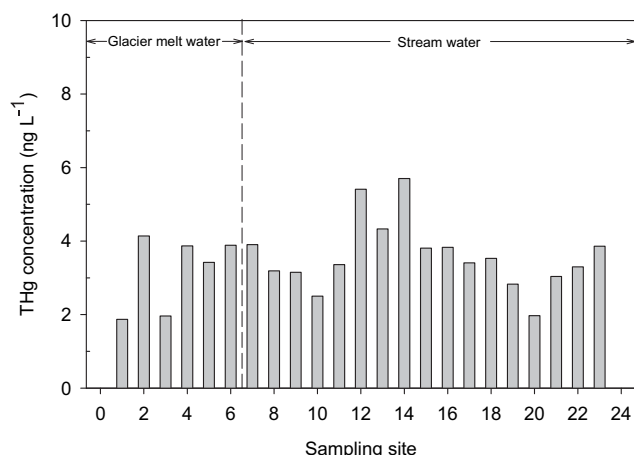
Fig. 7. Distribution of THg in glacier melt water and stream water in HNFP.

3.5. Input–output budget of THg in the HNFP

Input of THg to the upland forest of HNFP included wet (precipitation) and dry (net throughfall + litterfall) depositions (St. Louis et al., 2001; Graydon et al., 2006, 2009). Annual wet and dry deposition fluxes of THg in HNFP were 26.1 and 66.4 $\mu g\,m^{-2}\,yr^{-1}$, respectively. Assuming the area of HNFP was 151.9 km^2, the annual wet and dry deposition fluxes of THg were approximately 4.0 and 10.1 $kg\,yr^{-1}$, respectively, with a total mass flux of 14.1 $kg\,yr^{-1}$. Stream outflow and soil volatilization were the two major mechanisms for THg losses in the study area. Steam outflow of THg was estimated by multiplying the mean THg concentration in stream water (3.6 $ng\,L^{-1}$) and water discharge rate in the HNFP (annual water discharge: $3.72 \times 10^8\,m^3$, Lv and Wang, 2008). The export mass flux of THg via stream was 1.3 $kg\,yr^{-1}$ (outflow flux: 8.6 $\mu g\,m^{-2}\,yr^{-1}$). Soil volatilization of Hg was calculated to be 2.1 $kg\,yr^{-1}$ by multiplying the annual mean emission flux (14.0 $\mu g\,m^{-2}\,yr^{-1}$) and land area (151.9 km^2).

Input–output budget of THg in the study area and other study areas from literature are presented in Table 4. The study area was a net sink of THg, and the annual retention flux of THg reached 69.9 $\mu g\,m^{-2}\,yr^{-1}$. Dry deposition is the major pathway for THg loading to the upland forest, which was about 72% of the total inputs. On the other hand, evasion of Hg from forest soil played a more important role in THg outputs compared to stream outflow. By comparison, the annual loading of THg to HNFP was slightly higher than LGS and much lower than TSP in southwest China, but it was higher compared to some forest catchments in Europe and North America (Table 4). It should be pointed out that the models in Europe and North America did not estimate the THg losses via evasions, and therefore it is expected the elevated loading of THg to the HNFP compared to Europe and North America should be more pronounced. Since atmospheric Hg distributions in HNFP indicated impacts of heavy regional Hg emissions from industrial and urban areas (Fu et al., 2008a, 2009), we suppose anthropogenic emissions played important role in elevated loading of Hg to HNFP.

3.6. Distribution of THg in soil profiles

Total Hg and TOC content in the five soil profiles in the upland forest of HNFP are shown in Fig. 8. Aside from site P1 located in the alpine meadow (4200 m a.s.l.), THg concentrations in the study area showed a clear depth variation with relatively higher levels in the upper layers and lower levels in relatively deep layers ($p = 0.021$). It is discovered that the trend of THg concentrations in soil profile was highly correlated to soil TOC content (r^2 were 0.89, 0.90, 0.41, and 0.80 at P2, P3, P4, and P5, respectively.). This trend is in a good agreement with that observed in a national park of Minnesota (Wiener et al., 2006). As suggested by Wiener et al. (2006), highly elevated THg in forest surface soil was mostly likely attributed to atmospheric depositions via litterfall and throughfall, whereas the contribution from geological sources was very limited. However, P1 did not show a similar depth variation in THg concentrations and the surface soil concentration of THg at P1 was much lower than other sites. This indicates the enhancement of dry deposition of Hg to forest canopy followed by litterfall and throughfall.

Total Hg concentrations in topsoil in the forest of HNFP ranged from 0.12 to 0.26 $mg\,kg^{-1}$, which was comparable to results reported from other forest sites in China (Wang et al., 2006, 2008; Feng et al., 2006), but higher compared to those measured in forest soil in North America and Europe (e.g. St. Louis et al., 2001; Larssen et al., 2008; Biswas et al., 2008), and this is in a good agreement with the elevated loading of THg in the study area (Sect. 3.5).

Previous field and modeling studies have also found significant inputs of Hg to forest ecosystems and accumulation of Hg in forest soil (St. Louis et al., 2001; Selvendiran et al., 2008). In this study area, outflow of Hg via stream outflow and soil volatilization constituted a small portion of Hg budget in the study area. Therefore, there was very little loss of Hg from the forest soil and the accumulation of Hg in soil would be strengthened with time. However, the storage of mercury in forest soil could be re-emitted, and therefore represents an important risk. Organic carbon has a high affinity to Hg in soil, but the Hg bonded organic carbon would probably be released to the environment as the decomposition of organic matter occurs. Studies on climate change research have suggested that the increase of air temperature could accelerate the decomposition of organic carbon (Schimel et al., 1994), and therefore global warming could probably result in enhancement of Hg emission from soil (Obrist, 2007). In this study, we found the exchange flux of Hg between soil and atmosphere was

Table 4
Annual input and output flux of THg in the study area and literatures.

| Location	Input ($\mu g\,m^{-2}\,yr^{-1}$)			Output ($\mu g\,m^{-2}\,yr^{-1}$)			Sink ($\mu g\,m^{-2}\,yr^{-1}$)	Reference
	Wet deposition (of total input)	Dry deposition (of total input)	Total	Evasion (of total output)	Runoff (of total output)	Total		
HNFP, southwest China	26.1 (28.2%)	66.4 (71.8%)	92.5	14.0 (61.9%)	8.6 (38.1)	22.6	69.9	This study
LGS, south China	24.1 (20.1%)	95.4 (79.9%)	119.5	67.4 (95.7%)	3.0 (4.3%)	70.4	49.1	Wang et al., 2008
TSP, southwest China	45.2 (15.5%)	246 (84.5%)	291.2	73.6 (95.5%)	3.5 (4.5%)	77.1	214	
Lehstenbach, Germany	∼35 (64.8%)	∼19 (35.2%)	∼54	–	8	8	46	Schwesig and
Steinkreuz, Germany	28 (45.2%)	34 (54.8%)	62	–	3	3	59	Matzner, 2000
Svartberget, Sweden	7 (21.2%)	26 (78.8%)	33	–	1.6		–	Lee et al., 2000
Gårdsjőn, Sweden	10 (27.8%)	36 (72.2%)	36	–	1.8		–	
Champlain, USA	8.4 (18.9)	36 (81.1%)	44.4	–	2.7	2.7	41.7	Scherbatakoy et al., 1998
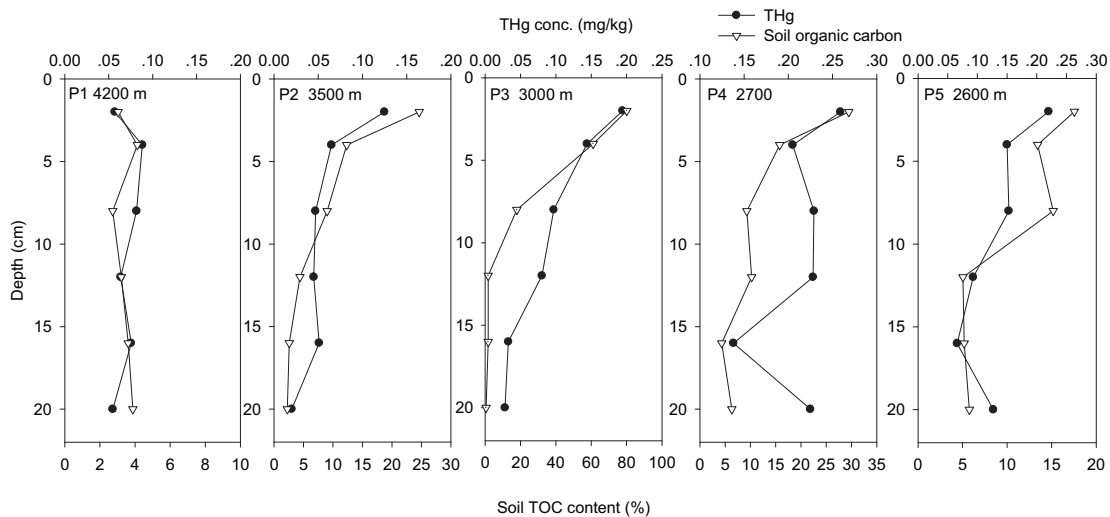
Fig. 8. THg distribution pattern in soil profiles in the upland forest of HNFP.

positively correlated with air temperature. Using the relationship established in Fig. 6, it is approximately estimated that the Hg emission flux could increase 2.7 μg m^{-2} yr^{-1} as the air temperature increases 1 °C.

4. Conclusions

Measurements of THg and MeHg depositions in precipitation and throughfall were carried out at an upland forest catchment in Hailuogou National Forest Park, southwest China from May 2005 to April 2007. Soil emission flux of Hg and distributions of THg in vegetation leaves, soil profiles and stream water were also investigated. Annual volume-weighted mean THg concentrations in precipitation, Emei fir forest throughfall and broad leaf Cuculidae forest throughfall were 14.3, 36.8 and 43.6 ng L^{-1}, respectively; and volume-weighted mean MeHg concentrations in precipitation and Emei fir forest throughfall and broad leaf Cuculidae forest throughfall were 0.16, 0.36 and 0.24 ng L^{-1}, respectively.

Input–output budget of THg elucidates that the upland forest in southwest China was a great sink of atmospheric Hg. The annual net input flux of THg reached 69.9 μg m^{-2} yr^{-1}. Dry deposition of Hg was the major pathway for Hg loading to the forest catchment, constituted about 71.8% of total input (92.5 μg m^{-2} yr^{-1}). Annual output of THg was 22.6 μg m^{-2} yr^{-1}, with 61.9% originating from soil evasion and 38.1% from stream outflow. The pool of THg in HNFP was much higher compared to remote forest catchments in Europe and North America, which was probably impacted by regional Hg emissions from industrial and urban areas.

References

Balogh, S.J., Huang, Y.B., Offerman, H.J., 2003. Methyl mercury in rivers draining cultivated watersheds. Science of Total Environment 304, 305–313.
Biswas, A., Blum, J.D., Keeler, G.J., 2008. Mercury storage in surface soil in a central Washington forest and estimated release during the 2001 Rex Creek fire. Science of Total Environment 404, 129–138.

Boudala, F.S., Folkins, I., Beauchamp, S., Tordon, R., Neima, J., Johnson, B., 2000. Mercury flux measurements over air and water in Kejimkujik national park, Nova Scotia. Water, Air and Soil Pollution 122, 183–202.
Bushey, J.T., Mallana, A.G., Montesdeoca, M.R., Driscoll, C.T., 2008. Mercury dynamics of a northern hardwood canopy. Atmospheric Environment 42, 6905–6914.
Choi, H.D., Sharac, T.J., Holsen, T.M., 2008. Mercury deposition in the Adirondacks: a comparison between precipitation and throughfall. Atmospheric Environment 42, 1818–1827.
Choi, H.D., Holsen, T.M., 2009. Gaseous mercury fluxes from the forest floor of the Adirondacks. Environmental Pollution 157, 592–600.
Coolbaugh, M.F., Gustin, M.S., Rytuba, J.J., 2002. Annual emissions of mercury to the atmosphere from natural sources in Nevada and California. Environmental Geology 42, 338–349.
De Vos, B., Van Meirvenne, M., Quataert, P., Deckers, J., Muys, B., 2005. Predictive quality of pedotransfer functions for estimating bulk density of forest soils. Soil Science Society of America Journal 69, 500–510.
Dvonch, J.T., Graney, J.R., Keeler, G.J., Stevens, R.K., 1999. Use of elemental tracers to source apportion mercury in South Florida precipitation. Environmental Science and Technology 33, 4522–4527.
Ericksen, J.A., Gustin, M.S., Xin, M., Weisberg, P.J., Fernadez, G.C.J., 2006. Air–soil exchange of mercury from background soils in the United States. Science of the Total Environment 366, 851–863.
Fang, F.M., Wang, Q.C., Li, J.F., 2004. Urban environmental mercury in Changchun, a metropolitan city in Northeastern China: source, cycle, and fate. Science of the Total Environment 330, 159–170.
Feng, X.B., Tang, S.L., Shang, L.H., Yan, H.Y., Zheng, W., 2004. Temporal variation of total gaseous mercury in the air of Guiyang, China. Journal of Geophysical Research 109, D03303. doi:10.1029/2003JD004159.
Feng, X.B., Dai, Q.J., Qiu, G.L., Li, G.H., He, L., 2006. Gold mining related mercury contamination in Tongguan, Shanxi Province, PR China. Applied Geochemistry 21, 1955–1968.
Feng, X.B., Jiang, H.M., Qiu, G.L., Yan, H.Y., Li, G.H., Li, Z.G., 2009a. Mercury mass balance study in Wujiangdu and Dongfeng reservoirs, Guizhou, China. Environmental Pollution 157, 2594–2603.
Feng, X.B., Jiang, H.M., Qiu, G.L., Yan, H.Y., Li, G.H., Li, Z.G., 2009b. Geochemical processes of mercury in Wujiangdu and Dongfeng reservoirs, Guizhou, China. Environmental Pollution 157, 2970–2984.
Fu, X.W., Feng, X.B., Zhu, W.Z., Wang, S.F., Lu, J., 2008a. Total gaseous mercury concentrations in ambient air in the eastern slope of Mt. Gongga, South-Eastern fringe of the Tibetan plateau, China. Atmospheric Environment 42, 970–979.
Fu, X.W., Feng, X.B., Zhu, W.Z., Zheng, W., Wang, S.F., Lu, J., 2008b. Total particulate and reactive gaseous mercury in ambient air on the eastern slope of the Mt. Gongga area, China. Applied Geochemistry 23, 408–418.
Fu, X.W., Feng, X.B., Wang, S.F., 2008c. Exchange fluxes of Hg between surfaces and atmosphere in the eastern flank of Mount Gongga, Sichuan province, south-western China. Journal of Geophysical Research 113, D20306. doi:10.1029/2008JD009814.
Fu, X.W., Feng, X.B., Wang, S.W., Rothenberg, R., Shang, L.H., et al., 2009. Temporal and spatial distributions of total gaseous mercury concentrations in ambient air in a mountainous area in southwestern China: implications for industrial and domestic mercury emissions in remote areas in China. Science of the Total Environment 407, 2306–2314.
Galloway, M.E., Branfireun, B.A., 2004. Mercury dynamics of a temperate forested wetland. Science of the Total Environment 325, 239–254.
Gillis, A.A., Miller, D.R., 2000. Some potential errors in the measurement of mercury gas exchange at the soil surface using a dynamic flux chamber. Science of the Total Environment 260, 181–189.

Graydon, J.A., St. Louis, V.L., Lindberg, S.E., Hintelmann, H., Krabbenhoft, D.P., 2006. Investigation of mercury exchange between forest canopy vegetation and the atmosphere using a new dynamic chamber. Environmental Science and Technology 40, 4680–4688.

Graydon, J.A., St. Louis, V.L., Hintelmann, H., Lindberg, S.E., Sandilands, K.A., et al., 2009. Long-term wet and dry deposition of total and methyl mercury in the remote boreal ecoregion of Canada. Environmental Science and Technology 42, 8345–8351.

Guo, Y.N., Feng, X.B., Li, Z.G., He, T.R., Yan, H.Y., et al., 2008. Distribution and wet deposition fluxes of total and methyl mercury in Wujiang reservoir Basin, Guizhou, China. Atmospheric Environment 42, 7096–7103.

Hall, B.D., St. Louis, V.L., 2004. Methlymercury and total mercury in plant litter decomposing in upland forests and flooded landscapes. Environmental Science and Technology 38, 5010–5021.

Hall, B.D., Manolopoulos, H., Hurley, J.P., Schauer, J.J., St. Louis, V.L., et al., 2005. Methyl and total mercury in precipitation in the Great Lakes region. Atmospheric Environment 39, 7557–7569.

Hartman, J.S., Weisberg, P.J., Pillai, R., Ericksen, J.A., Kuiken, T., et al., 2009. Application of a rule-based model to estimate mercury exchange for three background biomes in the continental United States. Environmental Science and Technology 43, 4989–4994.

Heiri, O., Lotter, A.F., Lemcke, G., 2001. Loss on ignition as a method for estimating organic and carbonate content in sediments: reproducibility and comparability of results. Journal of Paleolimnology 25, 101–110.

Keeler, G.J., Gratz, L.E., Al-Wali, K., 2005. Long-term atmospheric mercury et deposition at underhill, Vermont. Ecotoxicology 14, 71–83.

Landis, M.S., Keeler, G.J., 1997. Critical evaluation of a modified automatic wet-only precipitation collector for mercury and trace element determinations. Environmental Science and Technology 31, 2610–2615.

Landis, M.S., Keeler, G.J., 2002. Atmospheric mercury deposition to lake Michigan during the lake Michigan mass balance study. Environmental Science and Technology 36, 4518–4524.

Landis, M.S., Keeler, G.J., Al-Walib, K.I., Stevensc, R.K., 2004. Divalent inorganic reactive gaseous mercury emissions from a mercury cell chlor-alkali plant and its impact on near-field atmospheric dry deposition. Atmospheric Environment 38, 613–622.

Larssen, T., de Wit, H.A., Wiker, M., Halse, K., 2008. Mercury budget of a small forested boreal catchment in southeast Norway. Science of the Total Environment 404, 290–296.

Larssen, T., 2009. Mercury in Chinese reservoirs. Environmental Pollution 158, 24–25.

Lee, Y.H., Bishop, K.H., Menthe, J., 2000. Do concepts about catchment cycling of methylmercury and mercury in boreal catchments stand the test of time? Six years of atmospheric inputs and runoff export at Svartberget, northern Sweden. Science of the Total Environment 260, 11–20.

Lee, D.S., Nemitz, E., Fowler, D., Kingdon, R.D., 2001. Modelling atmospheric mercury transport and deposition across Europe and the UK. Atmospheric Environment 35, 5455–5466.

Lindberg, S.E., Stratton, W.J., 1998. Atmospheric speciation: concentrations and behavior of reactive gaseous mercury in ambient air. Environmental Science and Technology 32, 49–57.

Lindberg, S.E., Zhang, H., Vette, A.F., Gustin, M.S., Barnett, M.O., Kuiken, T., 2002. Dynamic flux chamber measurement of gaseous mercury emission fluxes over soils, Part 2: effect of flushing flow rate and verification of a two-resistance exchange interface simulation model. Atmospheric Environment 36, 847–859.

Lindberg, S.E., Bullock, R., Ebinghaus, R., Engstrom, D., Feng, X.B., et al., 2007. A synthesis of progress and uncertainties in attributing the sources of mercury in deposition. AMBIO 36, 19–32.

Liu, S.L., Nadim, F., Perkins, C., Carley, R.J., Hoag, G.E., Lin, Y., 2002. Atmospheric mercury monitoring survey in Beijing, China. Chemosphere 48, 97–107.

Luo, J., Yang, Z., Yang, Q.W., 2000. A study on the biomass and production of forest on the Gongga mountain. Acta Phytoecologica Sinica 24, 191–196 (in Chinese with abstract in English).

Lv, Y.X., Wang, G.X., 2008. Response of runoff variation to climate change in Hailuogou drainage basin in Gongga Mount in 1990–2007. Journal of Glaciology and Geocryology 30, 960–966 (in Chinese with abstract in English).

Lyons, W.B., Welch, K.A., Bonzongo, J.C., 1999. Mercury in aquatic systems in Antarctica. Geophysical Research Letter 26, 2235–2238.

Munthe, J., Hultberg, H., Lee, Y.H., Parkman, H., Iverfeldt, Å, et al., 1995. Trends of mercury and methylmercury in deposition, runoff water and sediments in relation to experimental manipulations and acidification. Water, Air, and Soil Pollution 85, 743–748.

Munthe, J., Lyvén, B., Parkman, H., Lee, Y.H., Iverfeldt, Å, et al., 2001. Mobility and methylation of mercury in forest soils development of an in-situ stable isotope tracer technique and initial results. Water, Air, and Soil Pollution 1, 385–393.

Obrist, D., 2007. Atmospheric mercury pollution due to losses of terrestrial carbon pools? Biogeochemistry 85, 119–123.

Oslo, Paris Commission, 1998. JAMP guidelines for the sampling and analysis of mercury in air and precipitation. Joint Assessment and Monitoring Programme 1998, 1–20.

Poissant, L., Pilote, M., Xu, X.H., Zhang, H., Beauvais, C., 2004. Atmospheric mercury speciation and deposition in the Bay St. Francois wetlands. Journal of Geophysical Research 109, D11301, doi:10.1029/2003JD004364.

Poissant, L., Pilote, M., Yumvihoze, E., Lean, D., 2008. Mercury concentrations and foliage/atmosphere fluxes in a maple forest ecosystem in Québec, Canada. Journal of Geophysical Research 113, D10307, doi:10.1029/2007JD009510.

Porvari, P., Verta, M., 2003. Total and methyl mercury concentrations and fluxes from small boreal forest catchments in Finland. Environment Pollution 123, 181–191.

Rea, A.W., Lindberg, S.E., Keeler, G.J., 2001. Dry deposition and foliar leaching of mercury and selected trace elements in deciduous forest throughfall. Atmospheric Environment 35, 3453–3462.

Rea, A.W., Lindberg, S.E., Scherbatskoy, T., Keeler, G.J., 2004. Mercury accumulation in foliage over time in two Northern mixed-hardwood forests. Water, Air, and Soil Pollution 133, 49–67.

Scherbatakoy, T., Shanley, J.B., Keeler, G.J., 1998. Factors controlling mercury transport in an upland forest catchment. Water, Air, and Soil Pollution 105, 427–438.

Schimel, D.S., Braswell, B.H., Holland, E.A., McKeown, R., Ojima, D.S., et al., 1994. Climatic, edaphic and biotic controls over storage and turnover of carbon in soils. Global Biogeochemical Cycles 8, 279–293.

Schroeder, W.H., Beauchamp, S., Edwards, G., Poissant, L., Rasmussen, P., et al., 2005. Gaseous mercury emissions from natural sources in Canadian landscapes. Journal of Geophysical Research 110, D18302, doi:10.1029/2004JD005699.

Schwesig, D., Matzner, E., 2000. Pools and fluxes of mercury and methylmercury in two forested catchments in Germany. Science of the Total Environment 260, 213–223.

Seigneur, C., Lohman, K., Vijayaraghavan, K., Shia, R.L., 2003. Contributions of global and regional sources to mercury deposition in New York State. Environmental Pollution 123, 365–373.

Selvendiran, P., Driscoll, C.T., Montesdeoca, M.R., Bushey, J.T., 2008. Inputs, storage, and transport of total and methyl mercury in two temperate forest wetlands. Journal of Geophysical Research 113, G00C01. doi:10.1029/2008JG000739.

Stamenkovic, J., Gustin, M.S., 2009. Nonstomatal and stomatal uptake of atmospheric mercury. Environmental Science and Technology 43, 1367–1372.

St. Louis, V.L., Rudd, W.M., Kelly, C.A., Hall, B.D., Rolfhus, K.R., et al., 2001. Importance of the forest canopy to flux of methylmercury and total mercury to boreal ecosystems. Environmental Science and Technology 35, 3089–3098.

US EPA, 1999. Method 1631: Revision B, Mercury in Water by Oxidation, Purge and Trap, and Cold Vapor Atomic Fluorescence Spectrometry. United States Environmental Protection Agency, pp. 1–33.

US EPA, 2001. Method 1630: Methyl Mercury in Water by Distillation, Aqueous Ethylation, Purge and Trap, and CVAFS.U.S. Environmental Protection Agency, Office of Water, Office of Science and Technology Engineering and Analysis Division (4303), 1200 Pennsylvania Avenue NW, Washington, DC 20460, pp. 1–41.

US National atmospheric deposition program, 2007. National atmospheric deposition program 2006 annual summary. http://nadp.sws.uiuc.edu/lib/data/2006as.pdf.

Valente, R.J., Shea, C., Humes, K.L., Tanner, R.L., 2007. Atmospheric mercury in the Great Smoky Mountains compared to regional and global levels. Atmospheric Environment 41, 1861–1873.

Vandal, G.M., Mason, P.R., McKnight, D., Fitzgerald, W., 1998. Mercury speciation and distribution in a polar desert lake (Lake Hoare, Antarctica) and two glacial meltwater streams. Science of the Total Environment 213, 229–237.

Wang, D.Y., He, L., Shi, X.J., Wei, S.Q., Feng, X.B., 2006. Release flux of mercury from different environmental surfaces in Chongqing, China. Chemosphere 64, 1845–1854.

Wang, S.F., Feng, X.B., Qiu, G.L., Fu, X.W., Wei, Z.Q., 2007. Characteristics of mercury exchange flux between soil and air in the heavily air-polluted area, eastern Guizhou, China. Atmospheric Environment 41, 5584–5594.

Wang, Z.W., Zhang, X.S., Xiao, J.S., Ci, Z.J., Yu, P.Z., 2008. Mercury fluxes and pools in three subtropical forested catchments, southwest China. Environmental Pollution 157, 801–808.

Wiener, J.G., Knights, B.C., Sandheinrich, M.B., Jeremiason, J.D., Brigham, M.E., et al., 2006. Mercury in soils, lakes and fish in Voyageurs National Park (Minnesota): importance of atmospheric deposition and ecosystem factors. Environmental Science and Technology 40, 6261–6268.

Westman, C.J., Hytonen, J., Wall, A., 2006. Loss-on-ignition in the determination of pools of organic carbon in soils of forests and afforested arable fields. Communications in Soil Science and Plant Analysis 37, 1059–1075.

Wu, Y., Wang, S.X., Streets, D.G., Hao, F.M., Chan, M., Jiang, J.K., 2007. Trends in anthropogenic mercury emissions in China from 1995 to 2003. Environmental Science and Technology 40, 5312–5318.

Zhang, H., Lindberg, S.E., Marsik, F.J., Keeler, K.J., 2001. Mercury air/surface exchange kinetics of background soils of the Tahquamenon river watershed in the Michigan upper peninsula. Water, Air, and Soil Pollution 126, 151–169.

Zhang, H., Lindberg, S.E., Barnett, M.O., Vette, A.F., Gustin, M.S., 2002. Dynamic flux chamber measurement of gaseous mercury emission fluxes over soils. Part 1: simulation of gaseous mercury emissions from soils using a two-resistance exchange interface model. Atmospheric Environment 36, 835–846.